Mem. S.A.It. Vol. 82, 648

Memorie della

Cosmic ray acceleration at weak cosmological shocks in test-particle regime

H. Kang[1] and D. Ryu[2]

[1] Department of Earth Sciences, Pusan National University, Pusan 609-735, Korea
e-mail: kang@uju.es.pusan.ac.kr
[2] Department of Astronomy and Space Science, Chungnam National University, Daejeon 305-764, Korea

Abstract. We examine the acceleration of cosmic-rays (CRs) via diffusive shock acceleration (DSA) at weak shocks in the test-particle regime. Assuming simple models for thermal leakage injection and Alfvénic drift, we first derive analytic solutions for accelerated particle spectra from both injected and pre-existing populations. We then compare these analytic solutions with the results from DSA simulations. If the Alfvén speed is comparable to the sound speed in the preshock flow, the power-law slope of CR spectrum can be significantly softer than the canonical test-particle slope, leading to lower injection rate and softer CR spectrum. Re-acceleration of pre-existing CRs dominates over the acceleration of injected particles at weak shocks, because thermal leakage injection becomes inefficient at low Mach number shocks in the adopted model. If the CR pressure in contributes to about 5 % of the thermal pressure in the upstream flow, the postshock CR pressure can increase to a few % of the shock ram pressure at shocks with $M \lesssim 3$, while it can reach up to 10 % for $M \sim 4-5$.

Key words. Cosmic rays – Shock waves – Particle acceleration

1. Introduction

Cosmological shock waves result from supersonic flow motions induced by hierarchical clustering during large-scale structure formation in the Universe. According to studies based on cosmological hydrodynamic simulations, the shocks formed by mergers of subclumps and internal flow motions inside the intracluster medium (ICM) of galaxy clusters are relatively weak with the characteristic Mach number, $M \sim 2-3$ (Ryu et al. 2003; Kang et al. 2007; Pfrommer et al. 2007; Skillman et al. 2008; Vazza et al. 2009). Indeed X-ray observations of shocks in merging clusters imply that the estimated shock Mach numbers are typically lower than 2-3 (Markevitch & Vikhlinin 2007).

The formation process of collisionless shocks in tenuous plasmas inevitably produces suprathermal particles, which can be further accelerated to very high energies through the interactions with resonantly scattering Alfvén waves in the converging flows across a shock, i.e. by diffusive shock acceleration (DSA) (Bell 1978; Drury 1983; Malkov & Drury 2001). The streaming motions of the high energy particles against the background fluid

Send offprint requests to: H. Kang

generate both resonant and nonresonant MHD waves upstream of the shock, which in turn scatter particles and amplify magnetic fields. Moreover, magnetic fields can be amplified by turbulence that is induced through cascade of vorticity generated behind curved shocks (Ryu et al. 2008). So it is natural to expect that structure formation shocks in the ICM generate CR electrons and protons and amplifies magnetic fields as well. The presence of magnetic fields of the order of μG and relativistic electrons have been inferred from observations of diffuse synchrotron emission from galaxy clusters (e.g., Carilli & Taylor 2002; Govoni & Feretti 2004, for review).

The CR pressure is expected to remain dynamically insignificant at weak shocks of $M \lesssim 5$, although there are highly nonlinear back-reactions from CRs to the underlying flow at strong shocks (Kang & Jones 2007). In the test-particle regime of the DSA theory, the post-shock CR spectrum takes a power-law $f(p) \propto p^{-q}$, where the spectral index depends on the velocity jump across the shock:

$$q = \frac{3(u_1 - v_A)}{u_1 - v_A - u_2}, \qquad (1)$$

where $u_1 = u_s$ and u_2 are the upstream and downstream flow speed, respectively, and $v_A = B_1/\sqrt{4\pi\rho_1}$ is the upstream Alfvén speed. This is based on the Alfvénic drift model in which scattering by Alfvén waves isotropizes the CR distribution in the wave frame (Skilling 1975). The Alfvénic drift in the upstream region reduces the velocity jump that the particles experience across the shock, which in turn softens the CR spectrum beyond the canonical test-particle slope. However, this effect is negligible for shocks with large Alfvénic Mach number, $M_A = u_s/v_A$. Hereafter, we use the subscripts "0", "1", and "2" to denote conditions far upstream, immediate upstream and downstream of the shock, respectively.

Using time-dependent DSA simulations with a thermal leakage injection model, we can find approximate, analytic solutions for the time-dependent CR spectrum in the test-particle regime (Kang & Ryu 2010). In this paper, we include the re-acceleration of pre-existing CRs by weak shocks, since the intergalactic gas is expected to first go through strong accretion shocks around nonlinear structures and then undergo weak merger shocks and internal flow shocks inside clusters of galaxies (Kang et al. 2007).

2. Analytic test-particle spectrum

In the test-particle limit of DSA theory, the CR proton spectrum has an exponential cutoff at

$$\frac{p_{\max}}{m_p c} \approx 10^8 \left(\frac{u_s}{10^3 \mathrm{kms}^{-1}}\right)^2 \left(\frac{t}{10^8 \mathrm{yrs}}\right) \left(\frac{B_0}{1\mu\mathrm{G}}\right), \qquad (2)$$

where t is the shock age, if the particles are confined around the shock without escape.

2.1. Injected CR population

At collisionless shocks suprathermal particles moving faster than the postshock thermal distribution may swim through the MHD waves and leak upstream across the shocks and get injected into the CR population (Malkov 1998; Kang et al. 2002). However it is not yet possible to make precise quantitative predictions for the CR injection process from first principles, because complex plasma interactions among CRs, waves, and the underlying gas flow are not fully understood yet (Malkov & Drury 2001). Here we adopt a phenomenological injection scheme in which particles above a certain injection momentum cross the shock and get injected into the CR population. The injection momentum $p_{\rm inj} = Q \cdot p_{\rm th}$ is parameterized with the parameter, $Q \sim 3 - 4$, where $p_{\rm th} = \sqrt{2 m_p k_B T_2}$ is the thermal peak momentum of the postshock gas. Thus the postshock CR spectrum due to the injected particles,

$$f_{\rm inj}(p) = f_{\rm th} \cdot (p/p_{\rm inj})^{-q} \exp(-qC), \qquad (3)$$

is anchored to the postshock Maxwellian distribution, where $f_{\rm th} = n_2 \pi^{-1.5}\, p_{\rm th}^{-3}\, \exp(-Q^2)$ and n_2 is the postshock proton number density. The cutoff function C is defined as

$$C(z) = \int_{z_{\rm inj}}^{z} \frac{dz'}{z'} \frac{1}{\exp(1/z') - 1}, \qquad (4)$$

where $z = p/(1.2 p_{\max})$ (Caprioli et al. 2009; Kang & Ryu 2010).

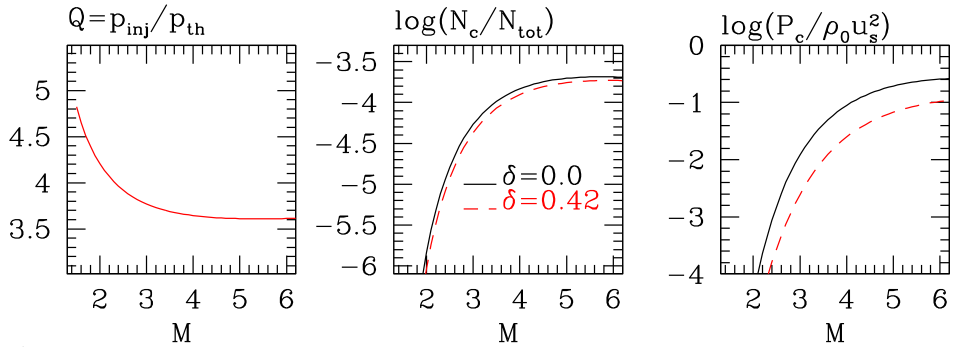

Fig. 1. The injection parameter Q adopted in this study, the fraction of CR particles and the postshock CR pressure at weak shocks propagating into the gas of $T_0 = 10^7$K. Models with two different values of Alfvén speed, $\delta = v_A/c_s$, are shown to illustrate the effect of Alfvénic drift.

Figure 1 shows the fraction of CR number and the ratio of the postshock CR pressure to the shock ram pressure for the analytic, test-particle spectrum given in Eq. (3). It shows that the models with Alfvénic drift ($\delta = 0.42$) have smaller CR pressure ($P_{c,2}/\rho_0 u_s^2 \lesssim 0.1$), compared to the models with $\delta = 0$, so they are indeed in test-particle regime.

2.2. Pre-existing CR population

When there is a upstream pre-existing CR population, with a spectrum $f_{\rm up}(p) = f_0(p/p_{\rm inj})^{-s}$, the re-accelerated CR spectrum in the steady-state limit is given by

$$f_{\rm dn}(p) = qp^{-q}\int_{p_{\rm inj}}^{p} p'^{q-1} f_{\rm up}(p')dp', \quad (5)$$

$$= \begin{cases} (\frac{q}{q-s})\left[1-(\frac{p}{p_{\rm inj}})^{-q+s}\right] f_{\rm up}(p), & \text{if } q \neq s \\ q\ln(p/p_{\rm inj}) f_{\rm up}(p), & \text{if } q = s \end{cases} \quad (6)$$

where the slope q is given in Eq. (1) (Drury 1983). If $q \neq s$, $f_{\rm dn}(p) \approx q/|s-q| \cdot f_0(p/p_{\rm inj})^{-r}$ for $p \gg p_{\rm inj}$, where $r = \min(q, s)$. Thus, if the pre-existing slope is softer than the test-particle slope (i.e. $s > q$), the re-accelerated CR spectrum gets flattened to p^{-q} by DSA. In the opposite case ($s < q$), the postshock CR spectrum is simply amplified by the factor $q/(q-s)$ and retains the same slope as the preshock slope.

Figure 2 illustrates the re-accelerated spectrum in the steady-state limit for a Mach 3 shock with $s = 4, 4.5, 5$. Note that the test-particle slope is $q = 4.5$ for $M = 3$ with $v_A = 0$. The time evolution of $f_{\rm dn}(p,t)$ from a DSA simulation is also shown for a upstream population of $f_{\rm up}(p) \propto p^{-5}$. This demonstrates that the time-dependent solutions (dotted lines) asymptotes to the steady-state solution (solid line). In the case of $s = 4$, the ratio, $f_{\rm dn}/f_{\rm up} \approx q/(q-s) = 9$, becomes constant for $p \gg p_{\rm inj}$.

In the time-dependent evolution, the re-accelerated spectrum should have the same cutoff as in the injected spectrum, as can be seen in Fig. 2. So the CR distribution at the shock location originated from both pre-existing and injected populations can be approximated by

$$f(p,t) \approx \left[f_{\rm dn}(p) + f_{\rm th}(p/p_{\rm inj})^{-q}\right] \exp\left[-qC\right] \quad (7)$$

3. DSA simulations

3.1. Simulation set-up

When the CR pressure is dynamically significant, typically for shock with $M \gtrsim 4$, the nonlinear feedback becomes important and the evolution of CR modified shocks should be followed by DSA simulations. Using our CRASH (Cosmic-Ray Acceleration SHock) code (Kang et al. 2002), we carried out kinetic DSA simulations, for a wide range of shock Mach numbers, $M = 1.5-5$. The diffusion-convection equation for $f(x,p,t)$ is solved along with suitably modified gasdynamic equations.

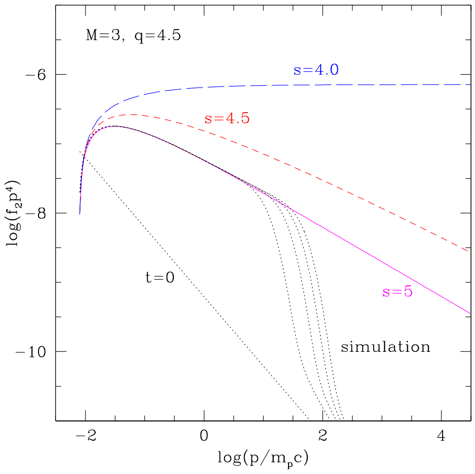

Fig. 2. Steady-state solutions given in Eq. (6) accelerated by a Mach 3 shock for the pre-existing CR spectrum, $f_{\rm up} \propto p^{-s}$ with $s = 4$ (long dashed line), 4.5 (dashed), 5 (solid). The dotted lines show the time-dependent solutions from the corresponding DSA simulation in the case $s = 5$.

We consider the shocks propagating into typical ICM of $T_0 = 10^7$K with the shock speed, $u_s = M \cdot 474\,{\rm km\,s^{-1}}$. The simulations start with a purely gasdynamic shock at rest at $x = 0$, initialized according to Rankine-Hugoniot relations with a gas adiabatic index, $\gamma_g = 5/3$. A Bohm-type diffusion coefficient, $\kappa(p) = \kappa^*(p/m_pc)(\rho_0/\rho)$, where $\kappa^*[m_pc^3/(3eB_0)]^{-1} = 10^{-3}$, is adopted for numerical convenience. Since the flow structure and the CR pressure P_c profile evolve self-similarly, a specific physical value of κ^* matters only in determination of $p_{\max}$ at a given shock age (Kang et al. 2009). For example, $p_{\max}/m_pc \approx 10^3$ is achieved by the termination time $t/t_o = 10$ in our simulations, where $t_o = \kappa^*/u_s^2$.

It is natural to assume the ICM contains pre-existing CRs, since the baryonic matter is heated by accretion shocks first and then by multiple internal shocks and merger shocks. Thus a upstream power-law CR population is specified with the amplitude, f_0, which is set by the upstream CR to gas pressure ratio, $R \equiv P_{c,0}/P_{g,0}$. Observations of nonthermal emission from galaxy clusters indicate that the CR proton pressure cannot exceed much more than ~ 10 % of the thermal pressure. So we consider the cases with $R = 0,\ 0.05$ and $s = 4,\ 4.5,\ 5$. The injection parameter, Q, and the fraction of injected particles, N_c/N_{tot}, are shown in Fig. 1.

To explore the effects of Alfvénic drift, we also adopt the Alfvén speed parameter, $\delta \equiv v_A/c_s = 0.42$ as a fiducial value, which corresponds to the case in which the magnetic field energy density is about 10 % of the thermal energy density, i.e. $E_B = 0.1E_{th}$.

3.2. CR proton spectrum and CR pressure

Figure 3 shows the postshock CR spectrum (left panels) and CR pressure (right panels) from the time-dependent DSA simulations with different model parameters. The results are shown for $t/t_o = 10$ when the shock evolution has reached the self-similar stage with steady values of $P_{c,2}$. The left panels demonstrate that the postshock CR spectrum from the DSA simulations can be well approximated by the analytic form in Eq. (7), i.e. combination of re-accelerated pre-existing CRs and freshly injected CRs with the exponential cutoff at $p_{\max}$. When there are no upstream CRs ($R = 0$, top panels), the CR injection and acceleration increase strongly with M. However, the re-acceleration of pre-existing particles dominates over the acceleration of injected particles, and enhances greatly the overall CR acceleration efficiency, especially at weaker shocks. Since the amplitude f_0 is larger for softer pre-existing spectrum, for the cases with $s = 5$ the re-acceleration becomes more important. For shocks with $M \lesssim 2$, both the CR injection and acceleration are very inefficient and the pre-existing CR spectrum is merely compressed by the shock without much acceleration.

In general, for fixed values of Q, R, and δ, the postshock CR pressure increases strongly with the shock Mach number. For shock with $M \gtrsim 4$, $P_{c,2}/(\rho_0 u_s^2) > 0.01$, consequently the nonlinear feedback may reduce slightly the CR injection and saturates the CR acceleration (Kang & Ryu 2010). As a result, $P_{c,2}$ in the DSA simulations (denoted by symbols) becomes smaller than the analytic estimates (lines) in the strictly test-particle limit for $M \gtrsim 4$. The comparison of the cases without ($\delta = 0$)

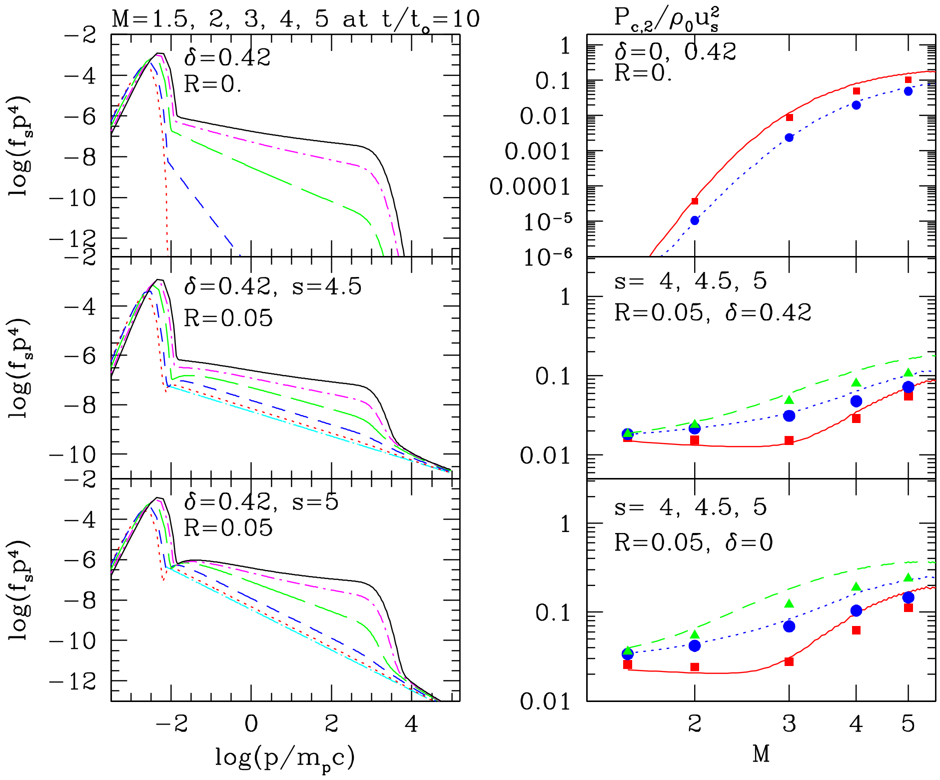

Fig. 3. *Left panels:* Postshock CR spectrum for shocks with M = 1.5 (dotted), 2 (dashed), 3 (long dashed), 4 (dot-dashed), and 5 (solid lines), and for different parameters, $R = P_{c,0}/P_{g,0}$ = 0, 0.05, the slope s = 4.5, 5, and the Alfvén speed $\delta = v_A/c_s$ = 0.42. *Right panels:* Postshock CR pressure in units of the shock ram pressure for different models. Lines show the analytic estimates calculated from $f(p,t)$ given in Eq. (7), while symbols show the results from the DSA simulations. In the top panel, squares are for δ = 0, while circles are for δ = 0.42. In the middle and bottom panels, squares are for s = 4, circles for s = 4.5 and triangles for s = 5.

and with (δ = 0.42) Alfvén speed illustrates the effect of Alfvénic drift, which softens the accelerated spectrum and reduces the CR pressure. The comparison of the cases with different pre-existing slope, s = 4 (solid lines), 4.5 (dotted), and 5 (dashed) shows that the CR acceleration is more efficient for softer preshock spectra (larger s). These results show that, for shocks with $M \lesssim 3$ the postshock CR pressure is typically a few % of the shock ram pressure even in the cases where the CR population takes up to 10 % of the thermal pressure in the upstream flow. For shocks with $M \sim 4-5$, these ratios can increase up to several 10 %. So we can safely adopt the test-particle solutions for these weak shocks in the ICM environment.

4. Summary

According to DSA theory for collisionless shocks, a small fraction of postshock thermal particles can be injected into the CR population, and then accelerated to high energies through their interactions with resonantly scattering Alfvén waves. Since the nonlinear DSA theory involves complex plasma and

MHD processes, it is not yet possible to derive accurate estimates for the CR injection and acceleration efficiencies from first principles. However, the analytic solutions presented here could provide simple yet reasonable approximations for weak shocks in test-particle regime. Here we adopt a thermal leakage injection model to emulate the acceleration of suprathermal particles into the CR population, as well as a simple transport model in which Alfvén waves self-excited by the CR streaming instability drift relative to the bulk plasma upstream of the gas subshock. We derive the analytic expression for the time-dependent CR spectrum in the test-particle regime, including both pre-existing and injected CR populations.

We also perform kinetic, time-dependent DSA simulations for a wide range of shock parameters including the shock Mach number (M), the slope of the preshock CR spectrum ($s = 4 - 5$), the ratio of the upstream CR pressure to gas pressure ($R = 0 - 0.05$), and the Alfvénic drift speed ($\delta = 0 - 0.42$). We then compare the results of the DSA simulations with the estimates based on the analytic form in Eq. (7). The main conclusions can be summarized as follows:

1) For weak shocks with $M \lesssim 3$, in which the CR injection is sufficiently low, the test-particle solution, $f(p,t)$, given in Eq. (7) should provide a good approximation for the time-dependent CR spectrum in the postshock region. For shock with $M \gtrsim 4$, $P_{c,2}/(\rho_0 u_s^2) > 0.01$ and the nonlinear feedback reduces slightly the CR injection and the CR acceleration saturates. As a result, $P_{c,2}$ in the DSA simulations becomes smaller than the analytic estimates based on the test-particle limit.

2) If there exist no CRs upstream ($R = 0$), the CR acceleration efficiency is less than 1% for $M \lesssim 3$, while it can reach to 1-10 % for $M \sim 4 - 5$. For the injection parameter Q considered here, the injection fraction is as low as $\xi \approx 10^{-6} - 10^{-3.7}$ for $2 \lesssim M \lesssim 5$. So the re-acceleration of pre-existing CRs dominates over the acceleration of freshly injected particles in most cases.

3) If the CR pressure is about 5 % of the thermal pressure in the upstream flow ($R = 0.05$), the postshock CR pressure can absorb about 1-10 % of the shock ram pressure for $M \lesssim 3$, depending on the upstream slope s and the Alfvén speed. The Alfvénic drift softens the CR spectrum and reduces the CR acceleration efficiency.

In summary, for weak cosmological shocks with $M \lesssim 3$, the CR acceleration efficiency cannot be much more than a few to 10 %, even with pre-existing CRs. Thus such shocks can be approximated by the test-particle solutions. On the other hand, shocks with $M \gtrsim 4$ may accelerate CRs with dynamically significant pressure.

Acknowledgements. HK was supported by National Research Foundation of Korea through grant 2009-0075060. DR was supported by National Research Foundation of Korea through grant 2007-0093860.

References

Bell, A. R. 1978, MNRAS, 182, 147
Carilli, C. L., & Taylor, G. B. 2002, ARA&A, 40, 319
Caprioli, D., Blasi, P., & Amato, E. 2009, MNRAS, 396, 2065
Drury, L. O'C. 1983, Rept. Prog. Phys., 46, 973
Govoni, F., & Feretti, L. 2004, Int. J. Mod. Phys. D, 13, 1549
Kang, H., Jones, T. W., & Gieseler, U. D. J. 2002, ApJ, 579, 337
Kang, H., & Jones, T. W. 2007, Astropart. Phys., 28, 232
Kang, H., & Ryu, D. 2010, ApJ, 721, 886
Kang, H., Ryu, D., Cen, R., & Ostriker, J.P. 2007, ApJ, 669, 729
Kang, H., Ryu, D., & Jones, T. W. 2009, ApJ, 695, 1273
Malkov M. A. 1998, Phys. Rev. E, 58, 4911
Malkov M. A., & Drury, L. O'C. 2001, Rep. Prog. Phys., 64, 429
Markevitch, M., & Vikhlinin, A. 2007, Phys. Rep., 443, 1
Pfrommer, C., Springel, V. Enßlin, T.A., & Jubelgas, M. 2007, MNRAS, 378, 385
Ryu, D., Kang, H., Hallman, E., & Jones, T. W. 2003, ApJ, 593, 599
Ryu, D., Kang, H., Cho, J., & Das, S. 2007, Science, 320, 909
Skilling, J. 1975, MNRAS, 172, 557
Skillman, S. W., et al. 2008, ApJ, 689, 1063
Vazza, F., Brunetti, G., & Gheller, C. 2009, MNRAS, 395, 1333